

## IDENTIFICATION AND REGULATION OF MECHANICAL IMPEDANCE FOR FORCE CONTROL OF ROBOT MANIPULATORS

T. Tsuji, K. Ito and H. Nagaoka  
Faculty of Engineering, Hiroshima University,  
Saijo-cho, Higashi-Hiroshima, Hiroshima, Japan

**Abstract.** Impedance control is one of the most powerful control methods for force control of manipulators. To apply the impedance control to actual tasks of the manipulators, there are several problems to be solved. The present paper discusses some of them, 1) the impedance identification of objects manipulated by robots, and 2) the impedance transformation from the task space into the joint space. For the first problem, we propose a new method which is able to identify the stiffness of the objects. It is based on the fact that the overall impedance at the contact point results as the sum of the object's impedance and the manipulator's one. Next, it is pointed out that the redundant manipulator allows to choose the joint impedance. Therefore for the second problem, we propose an impedance transformation method, which gives the closest joint impedance to the desired joint impedance in the least squared sense while satisfying the required end-point impedance.

**Keywords.** Impedance control ; robot ; force control ; motor control ; redundancy ; impedance transformation.

### INTRODUCTION

In robot control, it is essential to know how to control complex interactions between multi-joint arms and their environments. Some frequently cited tasks such as turning a crank, inserting a peg into a hole and opening a door, require not only position control of the manipulator's end-point but also force control in terms of the task space coordinates (Mason, 1981). For example, considering the task of rotating a crank, it's necessary that in a direction from the handle to the center of the rotation, the manipulator's end-point should be as compliant as possible, because in that direction the end-point trajectory of the manipulator is physically restricted by the handle trajectory of the crank. In a tangential direction of the crank, however, the position and/or velocity of the manipulator's end-point must be controlled to rotate the crank, because in that direction the manipulator can move freely.

This kind of compliance or rigidness of movement can be specified by mechanical impedance of the manipulators. The mechanical impedance provides the static and dynamic relationships between force and motion, and is a general term for stiffness, viscosity and inertia. Fine regulations of the mechanical impedance in multi-joint arms is one of the most important issues to perform the tasks which require interactions to their environments.

Hogan (1985a) proposed a concept of impedance control and showed that the position control and force control were simply degenerate and extreme cases of the impedance control. He also showed that multi-joint muscles and redundancy of joint degrees of freedom in human arms played important roles in fine regulation of its end-point impedance (Hogan, 1985b). Up to the present, several approaches to the impedance control of robot manipulators were proposed (Salisbury, 1980 ; Hogan, 1986, 1988 ; Khatib, 1987 ; Cutkosky, 1989). However, the fine impedance controller comparing with the human motor control system has not been developed, and several problems are remained to be solved. Some of them are as follows : (1) how to identify impedance characteristics of the environments, (2) how to determine the manipulator impedance in the task space, and (3) how to regulate the joint servo gains according to the given end-point impedance. Among them, the present paper discusses the first and the third one.

For the first problem, we propose a new method to identify the stiffness characteristics of the objects. And for the third one, we derive the impedance transformation from the end-point space to the joint space, using redundant joint degrees of freedom. This transformation procedure will be useful to solve the problems in terms of joint servo regulations. It is shown that the redundancy of the joint degrees of freedom allows to choose the impedance of each joint satisfying a desired end-point impedance.

### IMPEDANCE CONTROL OF ROBOT MANIPULATOR

#### Impedance in Multi-joint Arm

We consider a multi-joint arm having  $n$  joints. Let the position vectors in the joint and end-point coordinates be denoted as  $\theta \in R^n$  and  $X \in R^r$  respectively. Let also the corresponding force vectors be denoted as  $r \in R^n$  and  $F_e \in R^r$ , where  $n$  and  $r$  are the dimensions of the joint and end-point coordinates.

The transformation from  $\theta$  to  $X$  is nonlinear. The Jacobian matrix  $J$  is the locally linearized transformation matrix which is defined by (Asada and Clotire, 1986)

$$dX = J(\theta)d\theta. \quad (1)$$

Using the Jacobian matrix  $J$ , the transformation from  $F$  to  $r$  is given by

$$r = J^T F_e. \quad (2)$$

The Jacobian matrix  $J$  represents the link structures of the arm.

Impedance is a general term for stiffness, viscosity and inertia. Here, the stiffness in the joint coordinates and the end-point coordinates are defined. Note that the same holds for the viscosity. The stiffness matrices are given by

$$1) \text{ end-point level ; } F_e = -K_e dX \quad (3)$$

$$2) \text{ joint level ; } r = -K_j d\theta \quad (4)$$

where  $dX = X - X^e$  and  $d\theta = \theta - \theta^e$ .  $X^e$  and  $\theta^e$  are equilibrium points of the corresponding vectors. Using (1)-(4), we can obtain,

$$K_j = J^T K_c J, \quad (5)$$

which is called the active stiffness control (Salisbury, 1980).

### Impedance Control Law of Crank Rotation Task

We consider an impedance control taking a crank rotation as an example, which follows the active stiffness control (5).

First, let us define coordinates systems. Fig.1 shows a multi-joint manipulator and a crank. Assume that the rotation of the crank is restricted on the vertical plane ( $x-z$ ), and also the joint 0 and 4 of the manipulator are locked. Then, three coordinates systems are chosen as follows. Polar coordinates  $\Phi(\phi, r)$  with its origin at the center of the crank is defined as task coordinates. We also define Cartesian coordinates  $X(x, z)$  with its origin at the base of the manipulator as end-point coordinates of the manipulator. The manipulator also has joint coordinates  $\theta(\theta_1, \theta_2, \theta_3)$ . Note that the manipulator is redundant to the task space.

The nonlinear transformation from  $\Phi = (\phi, r)^T$  to  $X = (x, z)^T$  is defined as

$$X = g(\Phi). \quad (6)$$

Then we can obtain

$$dX = J_c(\Phi) d\Phi, \quad (7)$$

where, in this case

$$J_c = \begin{bmatrix} -r \sin \phi & \cos \phi \\ r \cos \phi & \sin \phi \end{bmatrix}. \quad (8)$$

Since the Jacobian matrix  $J_c$  is invertible, we can see

$$d\Phi = J_c^{-1} dX \quad (9)$$

$$F_c = (J_c^{-1})^T F_e, \quad (10)$$

where  $F_e$  and  $F_c$  are force vectors described in the end-point and task coordinates respectively.

Let us assume that an impedance control law in the task coordinates is written as

$$F_c = -K_t d\Phi - B_t \dot{d}\Phi, \quad (11)$$

where  $K_t \in R^{2 \times 2}$  is a desired task stiffness matrix,  $B_t \in R^{2 \times 2}$  is a desired task viscosity matrix,  $d\Phi = \Phi - \Phi^e$  and  $\dot{d}\Phi = \dot{\Phi} - \dot{\Phi}^e$ .  $\Phi^e$  and  $\dot{\Phi}^e$  are equilibrium points. Using (1)-(4) and (7)-(11), we may obtain the impedance control law in the joint coordinates,

$$\tau = -(J_c^{-1} J)^T K_t (J_c^{-1} J) d\theta - (J_c^{-1} J)^T B_t (J_c^{-1} J) \dot{d}\theta. \quad (12)$$

The above equation corresponds to the active stiffness control (5). Then, actuator control torque  $\bar{\tau}$  of the manipulator is given by

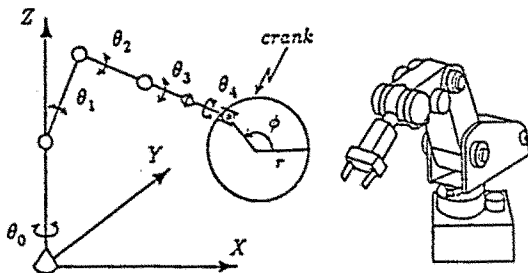


Fig.1 Crank rotation task by a manipulator.

$$\bar{\tau} = \tau + \Gamma(\theta, \dot{\theta}), \quad (13)$$

where  $\Gamma(\theta, \dot{\theta})$  is a compensation term of the gravity and joint friction torque.

The motion equation of the manipulator is given by

$$M(\theta)\ddot{\theta} + h(\theta, \dot{\theta}) + g(\theta) + v(\dot{\theta}) = \bar{\tau} + (J_c^{-1} J)^T F_{int}, \quad (14)$$

where,  $M(\theta)$  is non-singular inertia tensor,  $h(\theta, \dot{\theta})$  is Coriolis and centrifugal term,  $g(\theta)$  is the gravity term and  $v(\dot{\theta})$  is joint friction term.  $F_{int}$  is the external force to the end-point described in the task coordinates. Now, assume that the manipulator and the crank move slowly, and that the gravity and friction terms can be compensated by  $\Gamma(\theta, \dot{\theta})$ . In this case, the motion equation of the manipulator using the impedance control (12) reduces to the following equation

$$M_t(\theta)\ddot{\Phi} + B_t \dot{d}\Phi + K_t d\Phi = F_{int}, \quad (15)$$

where  $M_t(\theta)$  is inertia tensor in the task coordinates. Consequently it is clear that the desired task stiffness and viscosity can be achieved by the joint impedance control (12).

### Crank Rotation Experiments

The impedance control was applied to the actual manipulator. The stiffness matrix  $K_t$  and the viscosity matrix  $B_t$  are set as

$$K_t = \text{diag.} [0.5 \text{ (kgf}\cdot\text{m/rad)} \quad 10 \text{ (kgf/m)}], \quad (16)$$

$$B_t = \text{diag.} [0.25 \text{ (kgf}\cdot\text{m}\cdot\text{s/rad)} \quad 5 \text{ (kgf}\cdot\text{s/m)}], \quad (17)$$

where  $\text{diag.} [ \ ]$  means a diagonal matrix. The equilibrium point is  $\Phi^e = [ \pi/2 \text{ (rad)} \quad 0.15 \text{ (m)} ]^T$ .

At first, when the manipulator moves according to the control law (12) without grasping the handle of the crank, the disturbance force,  $f = 1 \text{ kgf}$ , is exerted to the manipulator's end-point in the direction of the arrow in Fig.2, showing one of the experimental results. It can be seen that the manipulator's end-point moves easily in response to the disturbance force.

Fig.3 shows an experimental result of the crank rotation task using the impedance control. Change of the manipulator configuration, and force vectors exerted to the crank by the manipulator are shown in Fig.3 (a) and (b) respectively. The force were measured by force sensors attached to the crank handle. If the manipulator's end-point impedance in the direction from the handle to the center of the crank is large, then a strong force is exerted to the crank by the manipulator due to the displacement error which may be caused by joint angle sensors and joint friction. We also tried a crank rotation task using position control. However it was impossible to rotate the crank

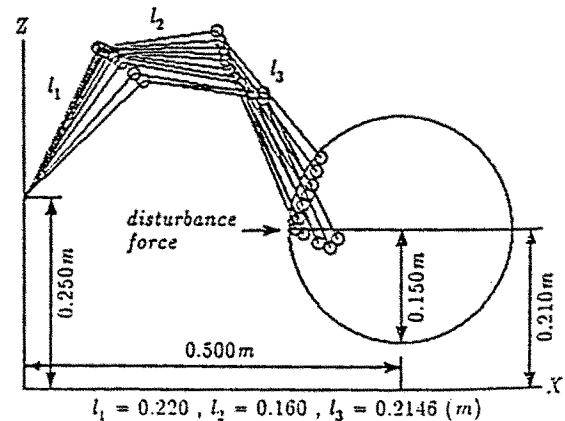


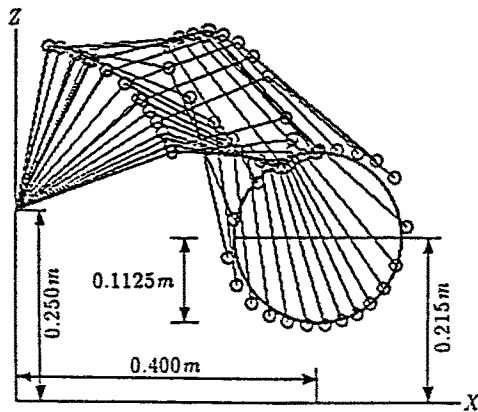
Fig.2 End-point displacements for a disturbance force (impedance control).

because of the strong force exerted to the crank handle. Consequently it is clear that the manipulator with the impedance controller can rotate the crank more smoothly and easily than the position controller.

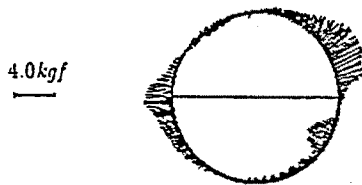
To establish the impedance control of robot manipulators, the following problems should be solved.

- (1) Impedance identification of environments : when the manipulator is in contact with an object such as a crank, the overall impedance is affected by not only the manipulator's end-point impedance but also the object impedance. In the experiments presented before, the crank impedance is assumed to be known. In general, identification of the impedance characteristics of the objects, such as a crank stiffness in terms of the task coordinates is required.
- (2) Determination of a desired impedance of the manipulator in the task space : according to the task and the object impedance, the manipulator's end-point impedance in the task space should be determined. In our experiments, it was determined by trial and error.
- (3) Impedance transformation from the task coordinates to the joint coordinates : servo gains associated with the joints contribute to the end-point impedance of the manipulator. This presents an inverse problem : adjusting the servo gains at the joints (the joint impedance) so as to achieve a desired end-point impedance. In the experiments presented before, we used the stiffness transformation (5) derived by Salisbury(1980). When the manipulator is redundant, however, this transformation always yields a singular joint stiffness matrix. It should be noted that the arm redundancy in the impedance transformation contributes to making impedance control more flexible.

In the following, we discuss the first and third problems among them.



(a) change of the arm posture



(b) force vectors exerted to the crank

Fig.3 Experimental results of a crank rotation task using impedance control.

## IMPEDANCE IDENTIFICATION OF OBJECTS

To determine an appropriate end-point impedance of manipulators according to a given task, first, we must consider impedance characteristics of the objects. For example, when we want to grasp a soft object or push it, we must check the mechanical characteristics such as stiffness, shape and mass of the object. Then we start to apply force to it. Consequently, to specify the manipulator impedance according to the needs of the task, we must establish an identification method of the objects' impedance characteristics. This is one of the most important issues to develop more autonomous and flexible manipulator control. We consider to identify the stiffness of an object because it is one of the most essential characteristics in the manipulation task.

### Identification Algorithm

Let us consider a case which an end-point of manipulator is in contact with an object, as shown in Fig.4. It is assumed that the manipulator rests in a joint angle  $\theta^e$  and that the stiffness  $K_{ob}$  and the direction  $\phi$  of the object are unknown. Let the overall stiffness at the contact point and the joint compliance of the manipulator be denoted as  $K_p$  and  $C_j$ , respectively. Since the contact of the manipulator's end-point with the object forms a parallel mechanism, the overall stiffness at the contact point is given by

$$K_p = K_{ob} + (JC_j J^T)^{-1}. \quad (18)$$

Consequently if we know the overall stiffness  $K_p$ , we can compute the object stiffness  $K_{ob}$ . In this case, we can estimate the stiffness and the direction of the object by the following procedure.

**Step 1 :** Preset an arbitrary nonsingular stiffness matrix  $K_j = C_j^{-1}$  and a viscosity matrix  $B_j$  to manipulator joints by adjusting joint servo gains. This is required for the directions which the object does not exist.

**Step 2 :** Estimate the overall joint compliance matrix  $\hat{C}_j$  which includes the effect of the object's stiffness :

$$\begin{bmatrix} d\theta_1 \\ d\theta_2 \\ \vdots \\ d\theta_m \end{bmatrix} = \begin{bmatrix} \hat{c}_{j11} & \hat{c}_{j12} & \cdots & \hat{c}_{j1m} \\ \hat{c}_{j21} & \hat{c}_{j22} & \cdots & \hat{c}_{j2m} \\ \vdots & \vdots & \ddots & \vdots \\ \hat{c}_{jm1} & \hat{c}_{jm2} & \cdots & \hat{c}_{jmm} \end{bmatrix} \begin{bmatrix} \tau_1 \\ \tau_2 \\ \vdots \\ \tau_m \end{bmatrix}. \quad (19)$$

**step 2-1 :** Set  $\hat{C}_j = C_j$  and  $i=1$ .

**step 2-2 :** The resultant joint displacements  $d\theta_i$  are measured, after applying the following torque  $\tau_i$  to the joint  $i$

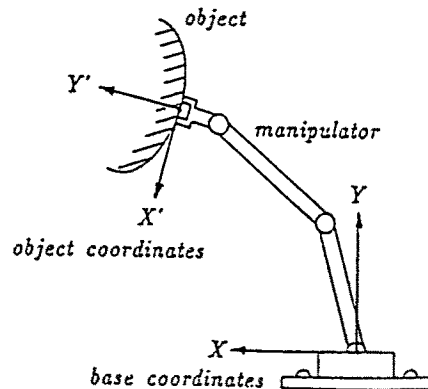


Fig.4 Manipulator in contact with an object.

$$\tau_i = \bar{\tau} \quad (20)$$

$$\tau_k = 0 \quad (k \neq i), \quad (21)$$

where  $\bar{\tau}$  is an arbitrary small torque.

step 2-3 : Compute the overall joint compliance  $\hat{c}_{jki}^*$  ( $k=1,2,\dots,m$ ) in Eq.(19).

step 2-4 : If  $\hat{c}_{jki}^*$  is different from the initial joint compliance  $c_{jki}$ , then  $\hat{c}_{jki}$  is replaced by  $\hat{c}_{jki}^*$ .

step 2-5 : If  $i=m$ , then go to step 2-6 ; otherwise set  $i=i+1$  and go to step 2-2.

step 2-6 : Set  $\bar{\tau} = -\bar{\tau}$  and repeat the procedure from step 2-2 to 2-4.

step 2-7 : If  $\hat{C}_j = C_j$ , it is supposed that the manipulator is not in contact with any object. Then the procedure is stopped.

**Step 3 :** Compute the overall contact point stiffness matrix in the base coordinates  $\hat{K}_p$  from the overall joint compliance  $\hat{C}_j$

$$\hat{K}_p = (J\hat{C}_jJ^T)^{-1}. \quad (22)$$

**Step 4 :** Compute the object stiffness matrix in the base coordinates

$$\hat{K}_{ob}^* = \hat{K}_p - (J\hat{C}_jJ^T)^{-1}. \quad (23)$$

**Step 5 :** Estimate the object stiffness matrix  $\hat{K}_{ob}^*$  in the object coordinates and the angle of rotation  $\hat{\phi}$  from the base coordinates to the object coordinates using the eigenvalues and eigenvectors of the matrix  $\hat{K}_{ob}^*$

$$\hat{K}_{ob}^* = T\Sigma T^T = R(\hat{\phi})\hat{K}_{ob}R^T(\hat{\phi}), \quad (24)$$

where  $T$  is an orthogonal matrix which each column is an eigenvector of  $\hat{K}_{ob}^*$  and  $\Sigma$  is a diagonal matrix which each element is an eigenvalue of  $\hat{K}_{ob}^*$ . Matrix  $T$  corresponds to a rotational matrix  $R(\hat{\phi})$  and Matrix  $\Sigma$  corresponds to a stiffness matrix of object  $\hat{K}_{ob}$ .

This procedure is only based on the measurement of the joint angles which are caused by joint torque perturbation. Note that it requires only joint torque controllers and angle sensors to implement this procedure. The force sensor at the end-point is not required.

### Simulation Experiment

A simulation experiment was performed using a three-link planar arm as shown in Fig.5, and the link parameters used in this experiment are shown in Table 1.

It is assumed that an object is purely elastic. The joint stiffness matrix  $K_j$  and the joint viscosity matrix  $B_j$  used in this experiment are

$$K_j = \text{diag.} [10.0 \ 10.0 \ 10.0] \quad (25)$$

$$B_j = \text{diag.} [5.0 \ 5.0 \ 5.0]. \quad (26)$$

We used the Newton-Euler method for the manipulator dynamics (Asada and Slotine, 1986).

Fig.6 shows the step responses of joint angle displacements  $d\theta_i$  ( $i=1,2,3$ ), when we apply torque  $\tau_1$  to the shoulder joint. Table 2 shows the simulation results. From Table 2, the estimated values of the object stiffness  $\hat{K}_{ob}^*$  and the object direction  $\hat{\phi}$  agree well with the true values.

To apply our method to actual tasks, we must take into account an effect of the measurement errors which may be caused by joint angle sensors, gravity force and joint friction. Further experiments using a real manipulator should be carried out. However, note that it is not necessary to estimate exactly the object impedance, because it depends on how to use the object impedance in the manipulator tasks.

Table 1 Link Parameters

	LINK 1	LINK 2	LINK 3
length(m) : $l_i$	0.30	0.24	0.11
mass(kg) : $m_i$	1.59	0.90	0.54
center of mass(m) : $l_{ci}$	0.162	0.125	0.055
moment of inertia : $I_i$ ( $\text{kg}\cdot\text{m}^2/\text{s}^2$ )	$1.58 \times 10^{-2}$	$4.76 \times 10^{-3}$	$5.87 \times 10^{-4}$

Table 2 Simulation Results of Impedance Identification

an object stiffness matrix in the object coordinates	
$K_{ob} = \begin{bmatrix} 0.1 & 0.0 \\ 0.0 & 100.0 \end{bmatrix}$	
a rotational matrix	
$R(\phi) = \begin{bmatrix} 0.1736484 & -0.9848077 \\ 0.9848077 & 0.1736484 \end{bmatrix}, \phi = 80.0$	
an estimated manipulator stiffness matrix	
$\hat{C}_j = \begin{bmatrix} 0.1031323 & -0.0631734 & -0.0097824 \\ -0.0631734 & 0.1587701 & -0.0064132 \\ -0.0097824 & -0.0064132 & 0.1989753 \end{bmatrix}$	
an estimated object stiffness matrix in the base coordinates	
$\hat{K}_{ob}^* = \begin{bmatrix} 96.9876543 & -17.0839900 \\ -17.0839628 & 3.1124635 \end{bmatrix}$	
an estimated object stiffness matrix in the object coordinates	
$\hat{K}_{ob} = \begin{bmatrix} 0.10008 & 0.0 \\ 0.0 & 100.00004 \end{bmatrix}$	
an estimated rotational matrix	
$R(\hat{\phi}) = \begin{bmatrix} 0.1736491 & -0.9848076 \\ 0.9848076 & 0.1736491 \end{bmatrix}, \hat{\phi} = 79.999946$	

nominal posture :  $\theta_1 = 10.0^\circ, \theta_2 = -70.0^\circ, \theta_3 = 35.0^\circ$

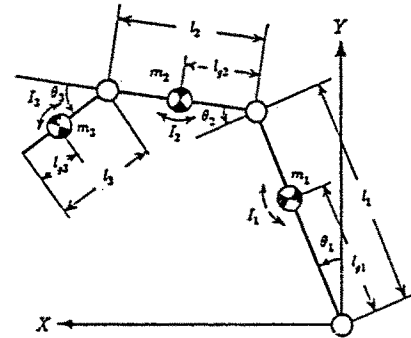


Fig.5 A three-link planar arm.

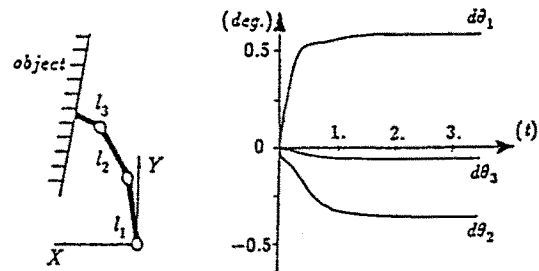


Fig 6 Step responses of joint angle displacements.

## IMPEDANCE TRANSFORMATION IN REDUNDANT ARM

The stiffness relationship between the joint and end-point coordinates is given by

$$K_j = J^T K_e J. \quad (27)$$

The corresponding transformation of compliance matrices is given by

$$C_e = J C_j J^T \quad (28)$$

where

$$C_e = K_e^{-1}, \quad (29)$$

$$C_j = K_j^{-1}. \quad (30)$$

Fig.7 shows the transformations between the force and displacement through the stiffness and compliance matrices.

If the stiffness matrix  $K_e$  is nonsingular in the end-point coordinates, the joint compliance matrix  $C_j$  seems to be computed from (27) and (30). However, if the manipulator is redundant such as the human arm, the impedance transformation between different levels brings a delicate issue. That is, even if  $K_e$  is nonsingular and Jacobian matrix  $J$  is of full row rank,  $K_j$  will be singular. Then  $C_j$  can not be computed from (30). Moreover, it should be noted that as the manipulator is redundant, the transformation of the end-point stiffness to the joint stiffness becomes an under-constrained problem (Tsuji, Ito and Nagamachi, 1988).

Let us consider the method to transform  $K_e$  into the joint stiffness  $K_j$ , when the end-point stiffness matrix  $K_e$  is given and is nonsingular. From (28) and (29), we can see

$$C_e = K_e^{-1} = J C_j J^T. \quad (31)$$

This implies that the transformation problem of stiffness or compliance is equivalent to solve the matrix equation (31) for the joint compliance matrix  $C_j$ .

The general solution of the matrix equation (31) is given by (see APPENDIX I)

$$C_j = J^+ C_e (J^+)^T + [Z - J^+ J Z (J^+)^T] \quad (32)$$

where  $Z \in R^{n \times n}$  is an arbitrary constant matrix and the superscript  $+$  denotes the Moore-Penrose generalized inverse (Whitney, 1972). Equation (32) means that the compliance of each joint can be arbitrarily specified through the matrix  $Z$  while satisfying the desired end-point impedance. Note that the same holds for the viscosity transformation.

It is remained to determine the arbitrary matrix  $Z$ . When  $Z$  is chosen as a zero matrix, the solution in (32) reduces to the minimum norm solution, that is to say, to minimize

$$\|C_j\| = \{ \text{tr} (C_j^T C_j) \}^{1/2} \quad (33)$$

where  $\text{tr}(A)$  means a trace of matrix  $A$ .

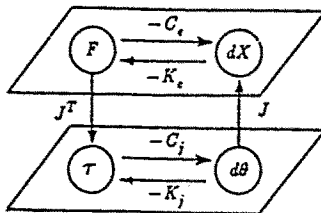


Fig.7 Stiffness relationship between joint and end-point coordinates.

Now, it is assumed that a desired joint compliance  $C_j^*$  is given according to a task. Then we consider to place  $C_j$  closest to  $C_j^*$  in the least squared sense. In this case, the goal is to find a matrix  $Z$  to minimize

$$\|C_j - C_j^*\| = \{ \text{tr} \{ (C_j^* - C_j)^T (C_j^* - C_j) \} \}^{1/2}. \quad (34)$$

This least squared problem can be solved (see APPENDIX II), yielding

$$Z = C_j^*. \quad (35)$$

Substituting (35) into (32), the final solution of the compliance transformation is given by

$$C_j = J^+ C_e (J^+)^T + [C_j^* - J^+ J C_e^* (J^+)^T]. \quad (36)$$

This solution gives the joint compliance  $C_j$  which is exactly transformed into the desired end-point compliance  $C_e^*$ , and is the closest one to the desired joint compliance  $C_j^*$ . It also implies that  $C_j$  usually will be nonsingular when  $C_j^*$  is nonsingular. Consequently we can immediately obtain the joint stiffness matrix  $K_j$ .

Table 3 shows the simulation results of stiffness transformation in a three-link planar arm (Fig.5). The end-point stiffness  $K_e$  is given as an identity matrix. In case 2, the compliance of wrist joint is larger than the shoulder and elbow joints. Conversely in case 3, the compliance of shoulder joint is larger than the others. Note that the end-point stiffness in all cases have an identity matrix and that each  $C_j$  in case 2 and 3 is a nonsingular matrix.

## CONCLUSION

In this paper, we discussed 1) the impedance identification of the objects manipulated by robots and 2) the impedance transformation from the task space into the joint space.

Corresponding to the first problem, we proposed the identification method of an object stiffness. It was shown that our identification method could estimate not only the object stiffness but also the object coordinates. For the second problem, we proposed the transformation method of the end-point impedance into the joint impedance. This method gave the closest impedance to the desired joint impedance in the least squared sense while satisfying the desired end-point impedance. The human arm also has redundancy (Mussa Ivaldi, 1986), and our transformation method can explain a part of the flexibility of human movements.

Future research will be directed to determine the task impedance appropriate to the specific tasks. This leads to the impedance planning problem and considered as one of the common problems in robot control and robot planning.

Table 3 Joint Compliance Matrices  
with the Same End-point Stiffness

	transformation matrix $Z$	joint compliance $C_j$
CASE 1	$\begin{bmatrix} 0.0 & 0.0 & 0.0 \\ 0.0 & 0.0 & 0.0 \\ 0.0 & 0.0 & 0.0 \end{bmatrix}$	$\begin{bmatrix} 12.4 & -4.4 & -4.8 \\ -4.4 & 9.3 & 4.9 \\ -4.8 & 4.9 & 3.2 \end{bmatrix}$
CASE 2	$\begin{bmatrix} 10.0 & 0.0 & 0.0 \\ 0.0 & 10.0 & 0.0 \\ 0.0 & 0.0 & 100.0 \end{bmatrix}$	$\begin{bmatrix} 9.3 & 0.69 & 0.45 \\ 0.69 & 9.3 & -4.0 \\ 0.45 & -4.0 & 93.3 \end{bmatrix}$
CASE 3	$\begin{bmatrix} 100.0 & 0.0 & 0.0 \\ 0.0 & 80.0 & 0.0 \\ 0.0 & 0.0 & 10.0 \end{bmatrix}$	$\begin{bmatrix} 20.8 & -17.0 & 12.2 \\ -17.0 & 27.9 & -17.0 \\ 12.2 & -17.0 & 0.01 \end{bmatrix}$

nominal posture :  $\theta_1 = -20^\circ$ ,  $\theta_2 = 10^\circ$ ,  $\theta_3 = 50^\circ$

## ACKNOWLEDGMENT

We would like to thank Takashi Ikemoto for computer simulation. The work presented in this paper was supported by the scientific research fund from the Ministry of Education under Grant #62460142(1987).

## REFERENCES

- Asada, H. and Slotine, J.J.E. (1986). *Robot Analysis and Control*, John Wiley & Sons, New York.
- Athans, M. (1967). The Matrix Minimum Principle. *Information and Control*, 11, 592-606.
- Cutkosky, M.R. (1989). Computing and Controlling the Compliance of a Robotic Hand. *IEEE Trans. Robotics and Automation*, 5, 151-165.
- Hogan, N. (1985a). Impedance Control; An Approach to Manipulation, Parts I, II, III. *Trans. the ASME J. of Dynamic Systems, Measurement and Control*, 107, 1-24.
- Hogan, N. (1985b). The Mechanics of Multi-Joint Posture and Movement. *Biol. Cybern.*, 53, 1-17.
- Hogan, N. (1986). Impedance Control Applied to Automated Debarring. In K.S. Narendra (Ed.). *Adaptive and Learning System*, Plenum Press, New York, 359-366.
- Hogan, N. (1988). On the Stability of Manipulators Performing Contact Tasks. *IEEE J. of Robotics and Automation*, 4, 677-686.
- Khatib, O. (1987). An Unified Approach for Motion and Force Control of Robot Manipulators: the Operational Space Formulation. *IEEE J. of Robotics and Automation*, 3, 43-53.
- Mason, M.T. (1981). Compliance and Force Control for Computer Controlled Manipulators. *IEEE Trans. System, Man and Cybernetics*, 11, 418-432.
- Mussa Ivaldi, F.A. (1986). Compliance, In P. Morasso and V. Tagliasco (Ed.). *Human Movement Understanding*, Elsevier, Amsterdam, 161-212.
- Salisbury, J.K. (1980). Active Stiffness Control of a Manipulator in Cartesian Coordinates. *Proc. 19th IEEE Conf. on Decision and Control*, 95-100.
- Tsuji, T. Ito, K. and Nagamachi, M. (1988). Motor Impedance Transformation in Multi-Joint Arm Movements. *IEEE EMBS 10th Int. Conf.*, 624-625.
- Whitney, D.E. (1972). The Mathematics of Coordinated Control of Prostheses and Manipulators, *Trans. ASME J. Dynamic Systems Measurement Control*, 94, 303-309.

## APPENDIX I

### The General Solution of Compliance Transformation

The general solution of the matrix equation (31) is given by

$$C_j = J^+ C_e (J^+)^T + [Z - J^+ J Z (J^+ J)^T] \quad (A-1)$$

proof. Substituting (A-1) into (31), we have

$$\begin{aligned} J C_j J^T &= J J^+ C_e (J J^+)^T + J [Z - J^+ J Z (J^+ J)^T] J^T \\ &= C_e \end{aligned} \quad (A-2)$$

Hence, it is clear that  $C_j$  in (A-1) is a solution of the matrix equation (31). On the other hand, let an arbitrary solution be denoted as  $S$ , then we can write

$$S = J^+ C_e (J^+)^T + [Z_1 - J^+ J Z_1 (J^+ J)^T] \quad (A-3)$$

where  $Z_1$  is defined by

$$Z_1 = S - J^+ C_e (J^+)^T \quad (A-4)$$

This completes the proof. ■

## APPENDIX II

### Least Squared Solution of Compliance Transformation

Substituting (32) into (34), we obtain the cost function

$$G(Z) = \left[ \text{tr} \left\{ (C_j^* - J^+ C_e (J^+)^T + Z - J^+ J Z (J^+ J)^T)^T (C_j^* - J^+ C_e (J^+)^T + Z - J^+ J Z (J^+ J)^T) \right\} \right]^2 \quad (A-5)$$

The problem is to find  $Z$  that satisfies equation (32) for a given  $C_e$  and  $J$  while minimizing the cost function  $G(Z)$ . The necessary condition that the optimal solution must satisfy is

$$\partial G(Z) / \partial Z = 0 \quad (A-6)$$

Substituting (A-5) into (A-6) and expanding it, we have

$$-C_j^* + J^+ J C_j^* J^+ J = -Z + J^+ J Z J^+ J \quad (A-7)$$

using the partial differential formulas about trace of matrices (Athans, 1967)

$$\partial \text{tr}(AX) / \partial X = A \quad (A-8)$$

$$\partial \text{tr}(X^T X) / \partial X = 2X \quad (A-9)$$

$$\partial \text{tr}(AXB) / \partial X = A^T B^T \quad (A-10)$$

$$\partial \text{tr}(A X^T B X C) / \partial X = B X C A + B^T X A^T C^T \quad (A-11)$$

and the properties of  $J^+$

$$(J^+ J)^T = J^+ J \quad (A-12)$$

$$(J^+ J)^T J^+ J = J^+ J \quad (A-13)$$

Consequently when we choose

$$Z = C_j^* \quad (A-14)$$

equation (A-7) holds clearly. Substituting the above into (32), we obtain

$$C_j = J^+ C_e (J^+)^T + [C_j^* - J^+ J C_j^* (J^+ J)^T] \quad (A-15)$$

It can be seen that the above equation satisfies the original compliance relationship (31) between the joint and the end-point coordinates.